ChemPlusChem

A Multidisciplinary Journal Centering on Chemistry

Accepted Article

Title: A Woven Supramolecular Metal-Organic Framework Comprising a Ruthenium Bis(terpyridine) Complex and Cucurbit[8]uril: Enhanced Catalytic Activity toward Alcohol Oxidation

Authors: Zhan-Ting Li, Yun-Chang Zhang, Zi-Yue Xu, Ze-Kun Wang, Hui Wang, Dan-Wei Zhang, and Yi Liu

This manuscript has been accepted after peer review and appears as an Accepted Article online prior to editing, proofing, and formal publication of the final Version of Record (VoR). This work is currently citable by using the Digital Object Identifier (DOI) given below. The VoR will be published online in Early View as soon as possible and may be different to this Accepted Article as a result of editing. Readers should obtain the VoR from the journal website shown below when it is published to ensure accuracy of information. The authors are responsible for the content of this Accepted Article.

WILEY-VCH

RESEARCH ARTICLE

A Woven Supramolecular Metal-Organic Framework Comprising a Ruthenium Bis(terpyridine) Complex and Cucurbit[8]uril: Enhanced Catalytic Activity toward Alcohol Oxidation

Yun-Chang Zhang,[a] Zi-Yue Xu,[a] Ze-Kun Wang,[a] Hui Wang,[a] Dan-Wei Zhang,*[a] Yi Liu,*[b] and Zhan-Ting Li*[a]

[a]   Dr. Y.-C. Zhang, Z.-Y. Xu, Z.-K. Wang, Prof. H. Wang, Prof. D.-W. Zhang, Prof. Z.-T. Li
        Department of Chemistry, Shanghai Key Laboratory of Molecular Catalysis and Innovative Materials
        Fudan University
        2205 Songhu Road, Shanghai 200438, China
        E-mail: zhngdw@fudan.edu.cn, ztli@fudan.edu.cn
[b]   Dr. Y. Liu
        Molecular Foundry
        Lawrence Berkeley National Laboratory
        One Cyclotron Road, Berkeley, California 94720, United States
        E-mail: yliu@lbl.gov

        Supporting information for this article is given via a link at the end of the document.

Abstract: The self-assembly of a diamondoid woven supramolecular metal organic framework **wSMOF-1** has been achieved from intertwined $[Ru(tpy)_2]^{2+}$ (tpy = 2,2',6',2"-terpyridine) complex **M1** and cucurbit[8]uril (CB[8]) in water through the encapsulation of CB[8] for intermolecular dimers formed by the appended aromatic arms of **M1**. **wSMOF-1** exhibits ordered pore periodicity in both water and the solid state, which is confirmed by a combination of ^{1}H NMR spectroscopy, UV-vis absorption, isothermal titration calorimetry, dynamic light scattering, small angle X-ray scattering and selected area electron diffraction experiments. The new woven framework has a pore aperture of 2.1 nm, which allows for the free access of both secondary and primary alcohols and tert-butyl hydroperoxide (TBHP). Compared with control molecule $[Ru(tpy)_2]Cl_2$, the $[Ru(tpy)_2]^{2+}$ unit of **wSMOF-1** exhibits a remarkably higher heterogeneous catalysis activity for the oxidation of alcohols by TBHP in n-hexane. For the oxidation of 1-phenylethan-1-ol, the yield of acetophenone was increased from 10% to 95%.

Introduction

Metal organic frameworks (MOFs) represent a family of regularly porous materials that consist of metal ions or clusters and bridging organic linkers.[1] The physical and chemical properties of MOFs are, to a considerable extent, dictated by the tunable porosity of the frameworks and the nature of the metal ions or clusters. Typically, the porosity endows the frameworks with remarkably amplified surface to allow for rapid, reversible entrance and exit of specific guests,[2,3] while the metal ions or clusters at the nodes provide periodically orientated sites for applications in, such as, catalysis,[4] sensing and imaging,[5] or drug delivery.[6] Following the reticular chemistry principles, MOFs are typically constructed by connecting metal ions with rigid bi- or multitopic molecular linkers. To expand the structural library of MOFs, several groups have reported the preparation of elegant interwoven MOFs through the crystallization of rationally designed coordination polymers.[7] However, assembling well-defined supramolecular polymers by weaving remains challenging,[8] and weaving in extended regular metal organic structures in solution is unexplored.

Cucurbit[8]uril (CB[8])-encapsulation-enhanced dimerization of aromatic units represents a robust approach for the construction of supramolecular polymers in water.[9] Through the co-assembly of preorganized multitopic molecular components and CB[8], we and other groups have constructed a variety of well-ordered two- and three-dimensional supramolecular organic frameworks (SOFs).[10] Previously, we reported that $[Ru(bpy)_3]^{2+}$(bpy: 2,2'-bipyridine)-derived hexatopic components interact with CB[8] to form porous MOF and SOF hybrids,[11] the $[Ru(bpy)_3]^{2+}$ of which exhibited enhanced electron-donating capacity upon photoexcitation for the reduction of protons to hydrogen. We here describe the first example of the supramolecular strategy for the synthesis of woven metal organic frameworks in water from an intertwined $[Ru(tpy)_2]^{2+}$ complex **M1** and CB[8]. We demonstrate that the regular arrangement of the $[Ru(tpy)_2]^{2+}$ units in the new woven supramolecular metal organic framework **wSMOF-1** leads to an important cage effect which remarkably increases their catalytic activity for the oxidation of primary and secondary alcohols.

Results and Discussion

To achieve the interweaving topology, ditopic terpyridine compound **3** was first prepared in 62% yield from the coupling reaction of compounds **1** and **2** (Scheme 1). Compound **3** was then reacted with ruthenium(DMSO) chloride to afford the tetratopic, water-soluble ruthenium complex **M1** in 92% yield. Molecular modelling showed that the aromatic backbone of the two ligands had an angle of intersection of 96.2° (Figure S1), while the whole complex produced a tetrahedral shape. The crystal structure (CCDC number: 1969587) of the complex between CB[8] and control **C1**,[12] which was prepared from the coupling reaction of **2** and 3-aminopyridine **4** (Scheme 1), confirmed a 1:2 binding motif with CB[8] encapsulating the anti-parallel 4-phenylpyiridinium dimer (Figure S2). ^{1}H NMR spectra in D_2O supported that this 1:2 binding stoichiometry also existed between **C1** and CB[8] in solution (Figure S3). In the presence of 2 equivalents of CB[8], the signals of free **C1** disappeared completely, while the complex gave rise to a set of signals of high

resolution for **C1**, which indicated selective formation of the expected three-component complex. Adding CB[8] to the solution of **M1** in D_2O caused rapid decrease of the resolution of the signals of **M1** in the ^{1}H NMR spectra (Figure S4). With the addition of 2 equivalents of CB[8], the signals in the downfield area nearly disappeared completely, which is diagnostic of the formation of supramolecular polymers. Adding CB[8] to the solution of **M1** in water also caused considerable hypochromism of the strongest absorption band of **M1** around 312 nm (Figure S5). This intensity change was dependent on the [CB[8]]/[**M1**] ratio, which displayed a clear inflection at [CB[8]]/[**M1**] = 2. This observation further confirmed the 2:1 binding stoichiometry between the 4-phenylpyridinium units of **M1** and CB[8]. Isothermal titration calorimetry afforded an apparent binding constant (K_a) of 4.0×10^{11} M^{-2} for this three-component complex (Figure S6), which was substantially higher than that of complex [**C1**]$_2$⊂CB[8] (1.4×10^{10} M^{-2}) (Figure S6). This difference clearly supported the presence of significant multivalence for the binding between the appended aromatic arms of **M1** and CB[8].[13] Dynamic light scattering (DLS) experiments revealed that the 1:2 solution of **M1** and CB[8] in water formed large aggregates, with the hydrodynamic diameter (D_H) ranging from 80 nm to 142 nm within the concentration range of 6 μM to 1.0 mM for **M1** (Figure S7). In contrast, the solution of **M1** (1.0 mM) and the 2:1 solution of **C1** (4.0 mM) and CB[8] formed much smaller aggregates, with D_H being 4.8 or 3.1 nm, respectively (Figure S7). These results again supported that the 1:2 mixture of **M1** and CB[8] afforded larger, extended supramolecular entities (Scheme 1).
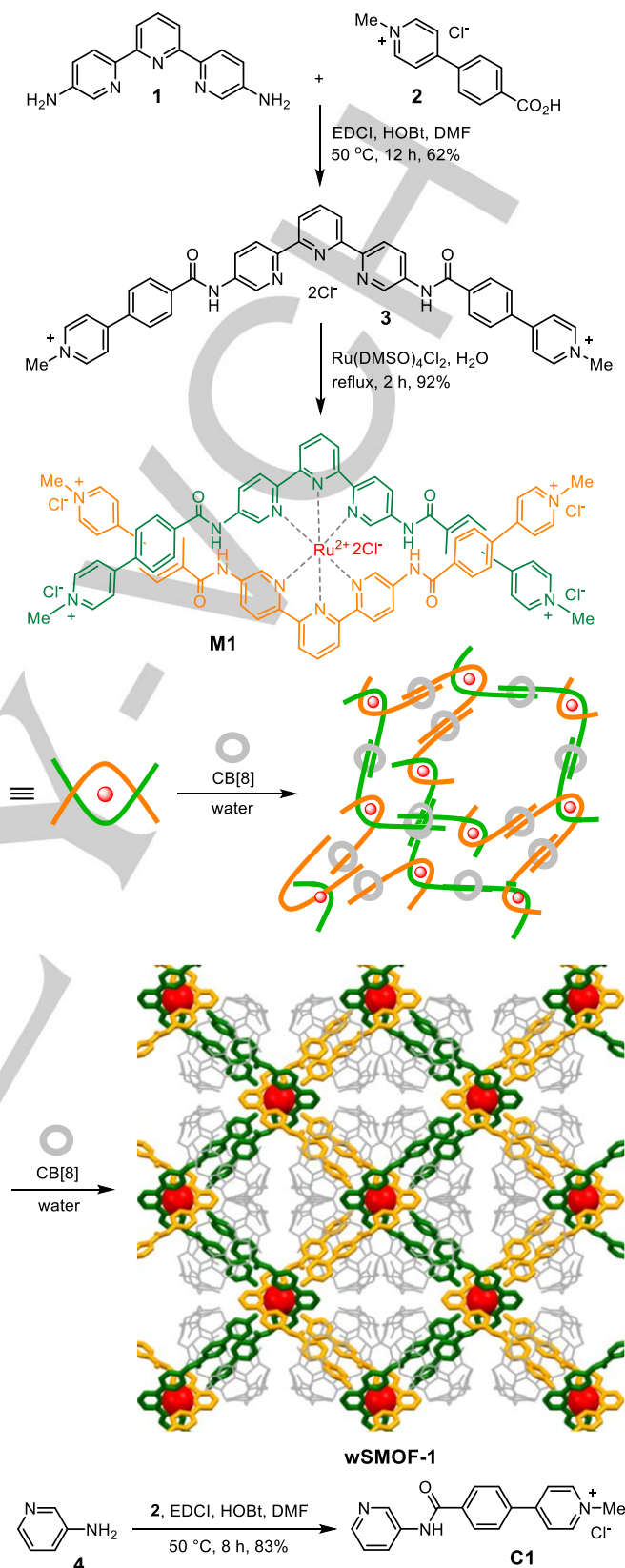

Scheme 1. The self-assembly of woven **wSMOF-1** and the preparation of **C1**.

The synchrotron small-angle X-ray scattering (SAXS) profile of the 1:2 solution of **M1** (1.0 mM) and CB[8] in water gave rise to a

RESEARCH ARTICLE

broad, but conspicuous peak around 1.8 nm (Figure 1a), which matched well with the calculated {202} spacing (1.8 nm) of the simulated woven supramolecular metal organic framework **wSMOF-1** (Scheme 1).[14] Upon slow evaporation, **wSMOF-1** precipitated as microcrystals. The synchrotron SAXS profile of the microcrystals displayed three sharper peaks, which centred at 2.0, 2.2 and 2.3 nm (Figure 1b), respectively, and correlated well with the calculated {211}, {201} and {200} spacings of **wSMOF-1**. The {211} and {200} spacings were also observed on the 2D profile (Figure 1b, inset). These observations supported that **wSMOF-1** formed the periodic woven structure in both water and the solid state. Transmission electron microscope (TEM) with the selected area electron diffraction (SAED) also confirmed the formation of the microcrystals, as the SAED pattern, that is, 1.8 nm for the {202} lattice spacing, was identical to the simulated value (1.8 nm). (Figure 1c). Elemental mapping analysis of the microcrystals further confirmed the composition of the C, N, O, Ru and Cl elements (Figure S8). Thermogravimetric analysis showed that **wSMOF-1** microcrystals had a good thermostability at up to 350 °C (Figure S9).
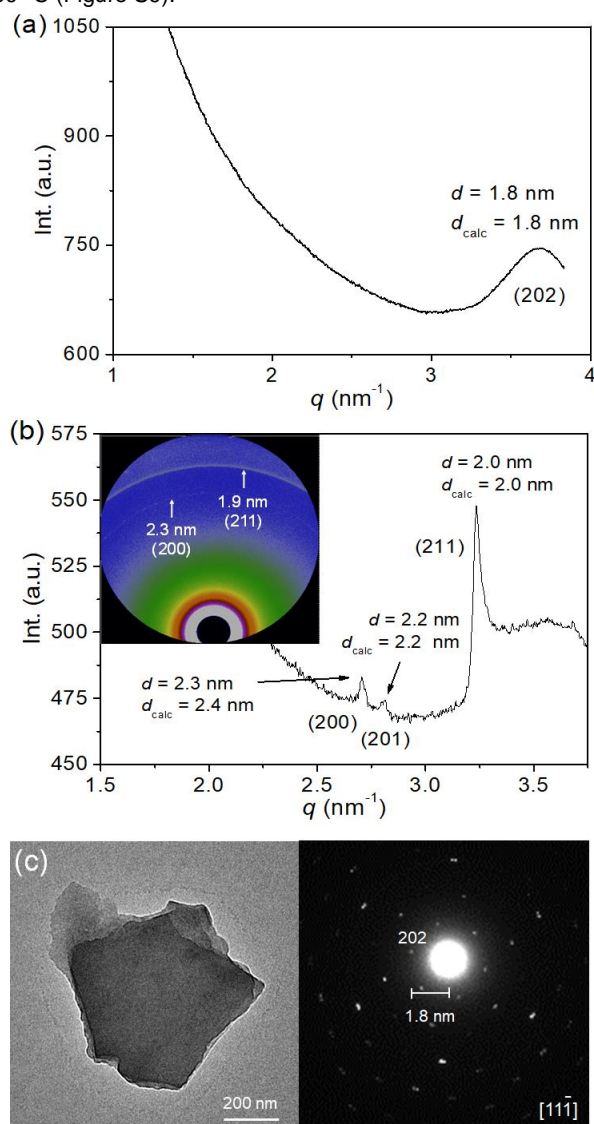
Figure 1. (a) Solution phase synchrotron SAXS profile of **wSMOF-1** ([**M1**] = 1.0 mM) in water, (b) synchrotron SAXS profile of **wSMOF-1** microcrystals (inset: 2D profile), and (c) TEM image of the microcrystal with the SAED pattern.

Structural modelling revealed that the diamondoid structure of **wSMOF-1** had a void volume of 78%, and the aperture, defined by six CB[8] macrocycles that formed a chair cyclohexane-like ring, was calculated to be about 2.1 nm. The $[Ru(tpy)_2]^{2+}$ complex is a well-known chromophore, but cannot function as an efficient photocatalyst due to its very short luminescent lifetime.[15] Since the $[Ru(tpy)_2]^{2+}$ units in **wSMOF-1** formed regular adamantane-like cages, we further investigated its potential as a catalyst through the possible cage enhancement effect.[16] As a proof of concept, we first chose to investigate the heterogeneous oxidation of secondary alcohols to the corresponding ketones, an important chemical transformation which can be realized using dyad photocatalysts where one or more $[Ru(tpy)_2]^{2+}$ units are attached to a $[Ru(tpy)(bpy)Cl]^+$ (bpy: 2,2'-bipyridine) catalytic unit.[17] All the reactions were conducted in *n*-hexane, with *tert*-butyl hydroperoxide (TBHP) as the oxidant in the presence of **wSMOF-1** microcrystalls with the molar amount of the $[Ru(tpy)_2]^{2+}$ units equaling 0.1 mole% of the substrates (Table 1). **wSMOF-1** was insoluble in nonpolar *n*-hexane, which was simply revealed by the fact that *n*-hexane containing the suspended **wSMOF-1** solid was colorless. Gas chromatography (GC) showed that all the studied alcohols **5a-j** were consumed completely within 3 h and the corresponding ketone products **6a-j** were obtained in excellent yields (92-95%), regardless of the existence of the electron-donating (entry 2) or withdrawing substituents (entries 3-5). With $[Ru(tpy)_2]Cl_2$ (0.1 mole%) as the heterogeneous control catalyst, after 3 h, GC analysis showed that ketones **6a-i** were obtained in a very low yield (Table 1), and most of the substrates were not converted. The highest yield (10%) of the ketone product **6a** was obtained from the oxidation of **5a**. The oxidation of **5a** with **M1** (0.1 mole%) as control heterogeneous catalyst was also conducted, which afforded **6a** in 6% yield. All these results supported that the Ru^{2+} complexes of **wSMOF-1** exhibited a significant cage effect through regular arrangement in the three-dimensional space. Compared with $[Ru(tpy)_2]Cl_2$, **wSMOF-1** with the same molar amount of the complex exhibited 9.5-fold (**5a**) to 31.7-fold (**5f**) efficiency enhancement. Notably, $[Ru(tpy)_2]Cl_2$ did not cause observable oxidation of **5j** after 3 h. In the absence of **wSMOF-1** or $[Ru(tpy)_2]Cl_2$, the above oxidation reactions did not take place. For **wSMOF-1**-catalyzed reaction of **5a** that was conducted in a darkroom, where indoor light was completely shielded, after 3 h, the alcohol product **6a** was obtained in a comparable yield (93%). This observation showed that the oxidation reaction was not photoinitiated. Thus, we propose a tentative mechanism for this reaction that involved the engagement of a seven-coordinated Ru^{2+} complex intermediate (Scheme 2), which has been established for many $[Ru(tpy)_2]^{2+}$-mediated photophysical and photochemical processes.[18] The $[Ru(tpy)_2]^{2+}$ complexes of **wSMOF-1** allowed for the formation of such unconventional seven-coordinated Ru^{2+} species probably due to the relatively weak and thus adaptable coordination of the tpy ligand to the Ru^{2+} ion.[19] The oxidation of **5a** was also performed in cyclohexane, dichloromethane, chloroform, acetonitrile or N,N-dimethylformamide under the same conditions, **6a** was produced in 93%, 88%, 90%, 87% or 86% yield, which was comparable or slightly lower than that obtained n-hexane. The catalyst was also insoluble in all these solvents, which was

3

RESEARCH ARTICLE

evidenced by the fact that the adsorption spectra of the suspended solution of the catalyst in these solvents did not exhibit any observable adsorption of the Ru^{2+} complex and thus reflected the good stability of the catalyst.

**Table 1. wSMOF-1**-catalyzed oxidation of secondary alcohols[a]

Entry	Substrate 5a-j	Product 5a-j	Conv. [%][b]	Yield
1	**5a**	**6a**	>99	95 (10)
2	**5b**	**6b**	>99	93 (6.5)
3	**5c**	**6c**	>99	94 (4.4)
4	**5d**	**6d**	>99	94 (6.1)
5	**5e**	**6e**	>99	94 (6.8)
6	**5f**	**6f**	>99	95 (3.0)
7	**5g**	**6g**	>99	92 (8.8)
8	**5h**	**6h**	>99	92 (7.7)
9	**5i**	**6i**	>99	95 (9.2)
10	**5j**	**6j**	>99	93 (0)

[a] The yields were determined by GC. [b] Values in the brackets are the yields using [Ru(tpy)$_2$]Cl$_2$ (0.1 mole%) as the catalyst.
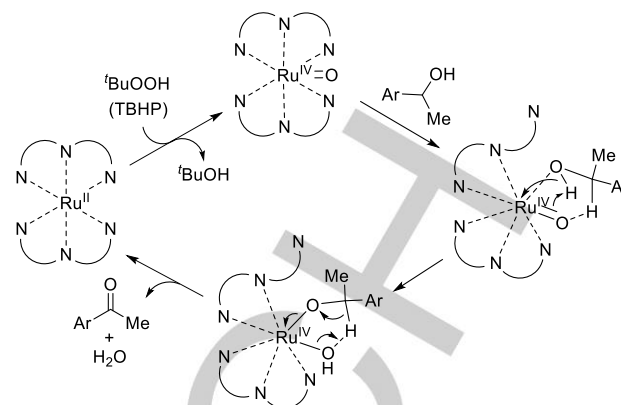
Scheme 2. The tentative mechanism for the **wSMOF-1**-catalyzed oxidation of **5a-j** to **6a-j** by TBHP. Compound **5a** was used as the reactant for illustration.

Given its high catalytic activity, the recyclability of **wSMOF-1** was then investigated for the oxidation of **5a**. The **wSMOF-1** catalyst could be readily recovered by simply centrifuging the suspension and washing the solid with *n*-hexane. It was found that, from ten cycled uses, GC analysis showed that ketone **6a** could be produced in 92-96% yields (Figure 2), which were comparable to that of the first turn (95%). Given analytical errors, these results supported that **wSMOF-1** fully maintained its catalytic activity through all the run of the reaction. The catalyst solid recovered after the tenth run was also subjected to the synchrotron SAXS measurement. The SAXS profile still gave rise to the peaks that corresponded to the {200}, {201} and {211} spacings, respectively (Figure S10), which indicated that the sample maintained its periodicity and reflected a high stability of the woven supramolecular architecture.
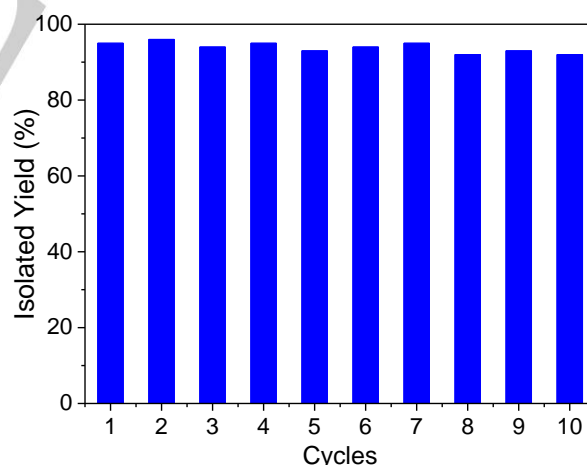
Figure 2. Isolated yield of acetophenone **6a** from the oxidation of 1-phenylethanol **5a** in *n*-hexane in the presence of TBHP (3.0 equiv.) and **wSMOF-1** (0.1 mole% relating to [Ru(tpy)$_2$]$^{2+}$) at 50 °C. The reaction time was 3 hours.

The catalysis of **wSMOF-1** for the oxidation of primary alcohols **7a-j** by TBHP was then further investigated. It was found that **wSMOF-1** effectively catalyzed the oxidation of all these alcohols (Scheme 3). Moreover, the reactions occurred also with no need of the induction of visible light. Under the catalysis of **wSMOF-1**,

4

all the ten studied alcohols were oxidized completely within 5 h. GC analysis indicated that no corresponding aldehydes were produced in detectable yields. Instead, the reactions gave rise to *tert*-butyl benzoperoxoates **8a-j** as well as the corresponding acids **9a-j**. The ratios of the two products depended on the substituent on the benzene ring of the substrates. The oxidation of **7a**, the benzene ring of which was substituent-free, afforded **8a** and **9a** in a comparable yield (49%). For **7b** and **7c** that bear an electron-donating substituent (Me or MeO) on the benzene ring, the corresponding acid was obtained as the major product. For **7d-j** that had an electron-withdrawing substituent on the benzene ring, all the reactions afforded *tert*-butyl benzoperoxoate as the major product. Although the formation of the acids could not be inhibited, they could be removed by easily washing the organic solution with an alkaline solution to afford the benzoperoxoates. Thus, this **wSMOF-1**-catalyzed oxidation reaction of benzyl alcohols by TBHP provides a new approach for the preparation of benzoperoxoates from primary alcohols.
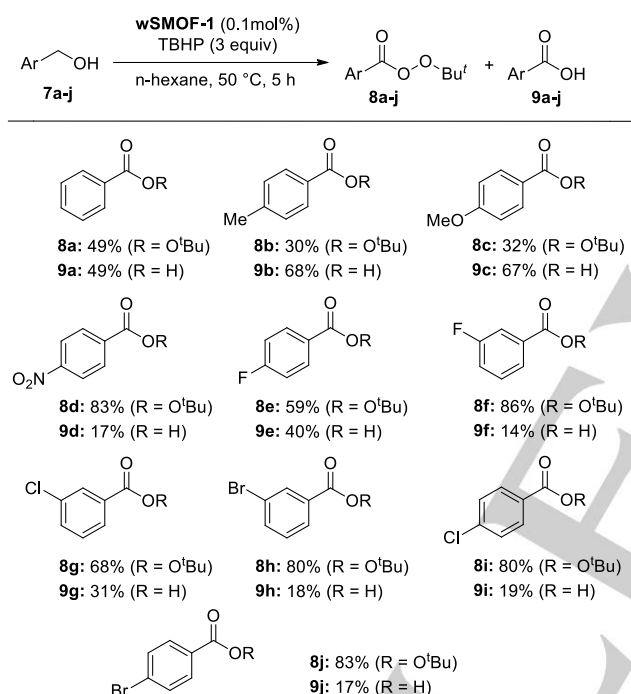
Scheme 3. wMOF-1-catalyzed oxidation of primary alcohols **7a-j** to produce **8a-j** and **9a-j**. The yields were determined by GC.

In the presence of **wSMOF-1**, the oxidations of benzaldehyde, 4-methylbenzldehyde and 4-nitrobenzaldehyde by TBHP in n-hexane were also conducted under the above conditions. The reactions afforded the corresponding *tert*-butyl benzoperoxoates and acids with a ratio comparable with that of the oxidation products of the related primary alcohols. These results supported that, for the oxidation of primary alcohols **7a-j**, both the *tert*-butyl benzoperoxoate and acid products were formed with the corresponding aldehyde as an intermediate. With [Ru(tpy)$_2$]Cl$_2$ as catalyst, the oxidation of **7a-j** by TBHP afforded the corresponding aldehydes in 4-26% yields (Figure S11). However, no corresponding *tert*-butyl benzoperoxoate or acid products were detected. We thus proposed a tentative mechanism for the formation of the *tert*-butyl benzoperoxoates and acids from the

primary alcohols that also involved the seven coordinated Ru^{2+} complex intermediates (Figure S12).

Conclusion

In summary, we have constructed a new woven supramolecular metal organic framework that exhibits ordered pore periodicity in water as well as the solid state. Weaving the ruthenium bis(terpyridine) complexes into the supramolecular metal organic framework leads to a remarkable cage effect through the introduction of regular pores. As a result, the woven ruthenium complexes display significantly enhanced catalytic activity for the oxidation of secondary and primary alcohols. This enhancement of catalysis activity suggests that transition metal complexes incorporated in a regular porous framework may accomplish new properties or functions that are not attained by the simple prototypic complexes, as reflected by the different products of the oxidation of aldehydes by the complex in the woven system and the control complex. Future research will focus on the introduction of other transition metals into woven frameworks and the design of new ligands for the development of woven MOFs that exhibit new topologies and properties as well as dynamic assembly behavior.

[1] a) H.-C. Zhou, J. R. Long, O. M. Yaghi, *Chem. Rev.* **2012**, *112*, 673–674; b) H.-C. J. Zhou, S. Kitagawa, *Chem. Soc. Rev.* **2014**, *43*, 5415–5418; c) A. J. Howarth, A. W. Peters, N. A. Vermeulen, T. C. Wang, J. T. Hupp, O. K. Farha, *Chem. Mater.* **2017**, *29*, 26–39; d) M. Y. Masoomi, A. Morsali, A. Dhakshinamoorthy, H. Garcia, *Angew. Chem.* **2019**, *131*, 15330–15347; *Angew. Chem. Int. Ed.* **2019**, *58*, 15188–15205.

[2] C. S. Diercks, M. J. Kalmutzki, N. J. Diercks, O. M. Yaghi, *ACS Central Sci.* **2018**, *4*, 1457–1464.

[3] a) J.-R. Li, R. J. Kuppler, H.-C. Zhou, *Chem. Soc. Rev.* 2009, *38*, 1477–1504; b) Y. He, F. Chen, B. Li, G. Qian, W. Zhou, B. Chen, *Coord. Chem. Rev.* **2018**, *373*, 167–198. c) J. Yu, L.-H. Xie, J.-R. Li, Y. Ma, J. M. Seminario, P. B. Balbuena, *Chem. Rev.* **2017**, *117*, 9674–9754.

[4] a) W. Lin, *J. Solid State Chem.* **2005**, *178*, 2486–2490; b) Q. Wang, D. Astruc, *Chem. Rev.* **2020**, *120*, 1438–1511; c) R. J. Drout, L. Robison, O. K. Farha, *Coord. Chem. Rev.* **2019**, *381*, 151–160; d) M. Liu, J. Wu, H. Hou, *Chem. Eur. J.* **2019**, *25*, 2935–2948; e) Y. Liu, W. Xuan, Y. Cui, *Adv. Mater.* **2010**, *22*, 4112–4135; f) K. Zhang, W. Guo, Z. Liang, R. Zou, *Sci. China Chem.* **2019**, *62*, 417–429; g) Z. Liang, C. Qu, D. Xia, R. Zou, Q. Xu, *Angew. Chem.* **2018**, *130*, 9750–9780; *Angew. Chem. Int. Ed.* **2018**, *57*, 9604–9633.

[5] a) B. Chen, S. Xiang, G. Qian, *Acc. Chem. Res.* **2010**, *43*, 1115–1124; b) A. Karmakar, P. Samanta, S. Dutta, S. K. Ghosh, *Chem. Asian J.* **2019**, *14*, 4506–4519; c) D. I. Osman, S. M. El-Sheikh, A. M. Salem, S. M. Sheta, O. I. Ali, W. G. Shousha, S. F. El-Khamisy, S. M. Shawky,

Biosensors Bioelectronics **2019**, *141*, 111451; d) J. Dong, D. Zhao, Y. Lu, W.-Y. Sun, *J. Mater. Chem. A* **2019**, *7*, 22744–22767; e) K. Chen, C. Wu, *Chin. Chem. Lett.* **2018**, *29*, 823–826; f) M. D. Allendorf, C. A. Bauer, R. K. Bhakta, R. J. T. Houk, *Chem. Soc. Rev.* **2009**, *38*, 1330–1352; g) J. Della Rocca, W. Lin, *Eur. J. Inorg. Chem.* **2010**, 3725–3734.

[6] a) R. C. Huxford, J. Della Rocca, W.-B. Lin, *Curr. Opin. Chem. Biol.* **2010**, *14*, 262–268; b) H. Cai, Y.-L. Huang, D. Li, *Coord. Chem. Rev.* **2019**, *378*, 207–221; c) W. Zhu, J. Zhao, Q. Chen, Z. Liu, *Chem. Rev.* **2019**, *398*, 113009; d) M.-X. Wu, Y.-W. Yang, *Adv. Mater.* **2017**, *29*, 1606134; e) L. He, Y. Liu, J. Lau, W. Fan, Q. Li, C. Zhang, P. Huang, X. Chen, *Nanomedicine* **2019**, *14*, 1343–1365.

[7] a) B. Chen, M. Eddaoudi, S. T. Hyde, M. O'Keeffe, O. M. Yaghi, *Science* **2001**, *291*, 1021–1023; b) N. C. Frank, D. J. Mercer, S. J. Loeb, *Chem. Eur. J.* **2013**, *19*, 14076–80; c) Y. He, Z. Guo, S. Xiang, Z. Zhang, W. Zhou, F. R. Fronczek, S. Parkin, S. T. Hyde, M. O'Keeffe, B. Chen, *Inorg. Chem.* **2013**, *52*, 11580–11584.

[8] a) M. C. T. Fyfe, J. F. Stoddart, *Coord. Chem. Rev.* **1999**, *183*, 139–155; b) K. C. Bentz, S. M. Cohen, *Angew. Chem.* **2018**, *130*, 15208–15218; *Angew. Chem. Int. Ed.* **2018**, *57*, 14992–15001.

[9] a) Y. H. Ko, E. Kim, I. Hwang, K. Kim, *Chem. Commun.* **2007**, 1305–1315; b) Y. Liu, H. Yang, Z. Wang, X. Zhang, *Chem. Asian J.* **2013**, *8*, 1626–1632; c) L. Isaacs, *Acc. Chem. Res.* **2014**, *47*, 2052–2062; d) J. Tian, L. Zhang, H. Wang, D.-W. Zhang, Z.-T. Li, *Supramol. Chem.* **2016**, *28*, 769–783; e) H. Zou, J. Liu, Y. Li, X. Li, X. Wang, *Small* **2018**, *14*, 1802234; f) Y. Chen, F. Huang, Z.-T. Li, Y. Liu, *Sci. China Chem.* **2018**, *61*, 979–992; g) J. del Barrio, J. Liu, R. A. Brady, C. S. Y. Tan, S. Chiodini, M. Ricci, R. Fernández-Leiro, C.-J. Tsai, P. Vasileiadi, L. D. Michele, D. Lairez, C. Toprakcioglu, O. A. Scherman, *J. Am. Chem. Soc.* **2019**, *141*, 14021–14025; h) E. Pazos, P. Novo, C. Peinador, A. E. Kaifer, M. S. García, *Angew. Chem. Int. Ed.* **2019**, *131*, 409–422; *Angew. Chem. Int. Ed.* **2019**, *58*, 403–416.

[10] a) K.-D. Zhang, J. Tian, D. Hanifi, Y. Zhang, A. C.-H. Sue, T.-Y. Zhou, L. Zhang, X. Zhao, Y. Liu, Z.-T. Li, *J. Am. Chem. Soc.* **2013**, *135*, 17913–17918; b) H. Zhang, F. Liang, Y.-W. Yang, *Chem. Eur. J.* **2020**, *26*, 198–205; c) H. Liu, Z. Zhang, Y. Zhao, Y. Zhou, B. Xue, Y. Han, Y. Wang, X. Mu, S. Zang, X. Zhou, Z. Li, *J. Mater. Chem. B* **2019**, *7*, 1435–1441; d) Q. Lin, Y.-Q. Fan, P.-P. Mao, L. Liu, J. Liu, Y.-M. Zhang, H. Yao, T.-B. Wei, *Chem. Eur. J.* **2018**, *24*, 777–783; e) S.-Q. Xu, X. Zhang, C.-B. Nie, Z.-F. Pang, X.-N. Xu, X. Zhao, *Chem. Commun.* **2015**, *51*, 16417–16420; f) M. Pfeffermann, R. Dong, R. Graf, W. Zajaczkowski, T. Gorelik, W. Pisula, A. Narita, K. Müllen, X. Feng, *J. Am. Chem. Soc.* **2015**, *137*, 14525–14532; g) H.-J. Lee, H.-J. Kim, E.-C. Lee, J. Kim, S. Y. Park, *Chem. Asian J.* **2018**, *13*, 390–394; h) Y. Li, Y. Dong, X. Miao, Y. Ren, B. Zhang, P. Wang, Y. Yu, B. Li, L. Isaacs, L. Cao, *Angew. Chem.* **2018**, *130*, 737–741; *Angew. Chem. Int. Ed.* **2018**, *57*, 729–733; i) J. Tian, T.-Y. Zhou, S.-C. Zhang, S. Aloni, M. V. Altoe, S.-H. Xie, H. Wang, D.-W. Zhang, X. Zhao, Y. Liu, Z.-T. Li, *Nat. Commun.* **2014**, *5*, 5574; j) S.-B. Yu, Q. Qi, B. Yang, H. Wang, D.-W. Zhang, Y. Liu, Z.-T. Li, *Small* **2018**, *14*, 1801037; k) B. Yang, X.-D. Zhang, J. Li, J. Tian, Y.-P. Wu, F.-X. Yu, R. Wang, H. Wang, D.-W. Zhang, Y. Liu, L. Zhou, Z.-T. Li, *CCS Chem.* **2019**, *1*, 156–165; l) Y.-P. Wu, Z.-K. Wang, H. Wang, D.-W. Zhang, X. Zhao, Z.-T. Li, *Acta Chim. Sinica* **2019**, *77*, 735–740; m) Y.-P. Wu, M. Yan, Z.-Z. Gao, J.-L. Hou, H. Wang, D.-W. Zhang, J. Zhang, Z.-T Li, *Chin. Chem. Lett.* **2019**, *30*, 1383–1386; n) M. Yan, W. Peng, H. Wang, D. Zhang, Z. Li, *Chin. J. Org. Chem.* **2019**, *39*, 2567–2573; o) M. Yan, X.-B. Liu, Z.-Z. Gao, Y.-P. Wu, J.-L. Hou, H. Wang, D.-W. Zhang, Y. Liu, Z.-T. Li, *Org. Chem. Front.* **2019**, *6*, 1698–1704; p) Z.-Z. Gao, Z.-K. Wang, L. Wei, G. Yin, J. Tian, C.-Z. Liu, H. Wang, D.-W. Zhang, Y.-B. Zhang, X. Li, Y. Liu, Z.-T. Li, *ACS Appl. Mater. Interfaces* **2020**, *12*, 1404–1411; q) H. Zhang, F. Liang, Y.-W. Yang, *Chem. Eur. J.* **2020**, *26*, 198–205.

[11] J. Tian, Z.-Y. Xu, D.-W. Zhang, H. Wang, S.-H. Xie, D.-W. Xu, Y.-H. Ren, H. Wang, Y. Liu, Z.-T. Li, *Nat. Commun.* **2016**, *7*, 11580.

[12] Deposition Number 1969587 (for complex (**C1**)$_2$⊂CB[8]) contains the supplementary crystallographic data for this paper. These data are provided free of charge by the joint Cambridge Crystallographic Data Centre and Fachinformationszentrum Karlsruhe Access Structures service www.ccdc.cam.ac.uk/structures.

[13] a) E. Mahon, M. Barboiu, *Org. Biomol. Chem.* **2015**, *13*, 10590–10599; b) J.-F. Xu, L. Chen, X. Zhang, *Chem. Eur. J.* **2015**, *21*, 11938–11946.

[14] Materials Studio 7.0, Accelrys Software Inc., San Diego, USA. 56.

[15] A. Juris, V. Balzani, F. Barigelletti, S. Campagna, P. Belser, A. von Zelewsky, *Coord. Chem. Rev.* **1988**, *84*, 85–277.

[16] a) X.-F. Li, S.-B. Yu, B. Yang, J. Tian, H. Wang, D.-W. Zhang, Y. Liu, Z.-T. Li, *Sci. China Chem.* **2018**, *61*, 830–835; b) X.-F. Li, X.-B. Liu, J.-Y. Chao, Z.-K. Wang, F.-U. Rahman, H. Wang, D.-W. Zhang, Y. Liu, Z.-T. Li, *Sci. China Chem.* **2019**, *62*, 1634–1638.

[17] a) W. Chen, F. N. Rein, R. C. Rocha, *Angew. Chem. Int. Ed.* **2009**, *48*, 9672–9675; b) D. Chao, W.-F. Fu, *Chem. Commun.* **2013**, *49*, 3872–3874.

[18] R. Matheu, M. Z. Ertem, C. Gimbert-Suriñach, X. Sala, A. Llobet, *Chem. Rev.* **2019**, *119*, 3453–3471.

[19] A. Soupart, I. M. Dixon, F. Alary, J.-L. Heully, *Theor. Chem. Acc.* **2018**, *137*, 37.

6

WILEY-VCH

RESEARCH ARTICLE

Entry for the Table of Contents
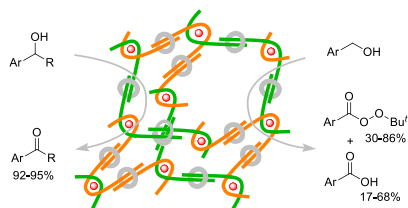
A woven supramolecular metal organic framework is assembled from an intertwined [Ru(tpy)$_2$]$^{2+}$ complex and cucurbit[8]uril. Regularly weaving the [Ru(tpy)$_2$]$^{2+}$ units into the supramolecular metal organic framework leads to a significant cage effect, which enables the intrinsically low-activity complexes to exhibit remarkably high catalytic activity for the oxidation of primary and secondary alcohols. For the oxidation of secondary alcohols, the yields of the corresponding ketones can be increased from ≤10%, obtained with [Ru(tpy)$_2$]$^{2+}$ control, to ≥92%.